Toxicology and Applied Pharmacology 272 (2013) 356–364

Contents lists available at ScienceDirect

Toxicology and Applied Pharmacology

journal homepage: www.elsevier.com/locate/ytaap

Tumor cell death induced by the inhibition of mitochondrial electron transport: The effect of 3-hydroxybakuchiol

Fabián Jaña [a], Francesca Faini [c], Michel Lapier [a], Mario Pavani [a], Ulrike Kemmerling [b], Antonio Morello [a], Juan Diego Maya [a], José Jara [a], Eduardo Parra [d], Jorge Ferreira [a,*]

[a] Clinical & Molecular Pharmacology Program, University of Chile, Santiago, Chile
[b] Anatomy and Developmental Biology Program, ICBM, Faculty of Medicine, University of Chile, Santiago, Chile
[c] Department of Chemistry, Faculty of Sciences, University of Chile, Santiago, Chile
[d] Laboratory of Experimental Biomedicine, University of Tarapaca, Campus Esmeralda, Iquique, Chile

ARTICLE INFO

Article history:
Received 8 March 2013
Revised 29 May 2013
Accepted 7 June 2013
Available online 15 June 2013

Keywords:
3-hydroxybakuchiol
Electron transport chain
Apoptosis
Mitochondria

ABSTRACT

Changes in mitochondrial ATP synthesis can affect the function of tumor cells due to the dependence of the first step of glycolysis on mitochondrial ATP. The oxidative phosphorylation (OXPHOS) system is responsible for the synthesis of approximately 90% of the ATP in normal cells and up to 50% in most glycolytic cancers; therefore, inhibition of the electron transport chain (ETC) emerges as an attractive therapeutic target. We studied the effect of a lipophilic isoprenylated catechol, 3-hydroxybakuchiol (3-OHbk), a putative ETC inhibitor isolated from *Psoralea glandulosa*. 3-OHbk exerted cytotoxic and anti-proliferative effects on the TA3/Ha mouse mammary adenocarcinoma cell line and induced a decrease in the mitochondrial transmembrane potential, the activation of caspase-3, the opening of the mitochondrial permeability transport pore (MPTP) and nuclear DNA fragmentation. Additionally, 3-OHbk inhibited oxygen consumption, an effect that was completely reversed by succinate (an electron donor for Complex II) and duroquinol (electron donor for Complex III), suggesting that 3-OHbk disrupted the electron flow at the level of Complex I. The inhibition of OXPHOS did not increase the level of reactive oxygen species (ROS) but caused a large decrease in the intracellular ATP level. ETC inhibitors have been shown to induce cell death through necrosis and apoptosis by increasing ROS generation. Nevertheless, we demonstrated that 3-OHbk inhibited the ETC and induced apoptosis through an interaction with Complex I. By delivering electrons directly to Complex III with duroquinol, cell death was almost completely abrogated. These results suggest that 3-OHbk has antitumor activity resulting from interactions with the ETC, a system that is already deficient in cancer cells.

Introduction

One of the most significant modifications that occur in cancer cells is the "Warburg Effect," the shift from oxidative phosphorylation (OXPHOS) to aerobic glycolysis for ATP generation as the cell's main source of energy (Vander Heiden et al., 2009). Several studies have shown that in cancer cells, some glycolytic enzyme isoforms are overexpressed. Among them, hexokinase II isoform (HKII) favors the glycolytic pathway in cancer cells. HKII has a high affinity for glucose and is attached to the voltage-dependent anion channel (VDAC) on the outer mitochondrial membrane. This location prevents the inhibition of this enzyme by its product, glucose-6-P, and provides preferential access to mitochondrial ATP (Pedersen, 2012). Thus, there is an important link between glycolysis and mitochondrial function. Consequently, the synthesis of ATP from OXPHOS remains critical.

There are several differences between the mitochondria in normal cells and those in tumor cells (Gatenby and Gillies, 2004; Kroemer and Pouyssegur, 2008), including differences in the preference of respiratory substrates, electron flow rate, the transport of anions and the ability to accumulate and retain calcium (DeBerardinis and Cheng, 2010). Certain key enzyme activities involved in OXPHOS are strongly decreased in cancer cells. For example, the activities of the F1β subunit of ATP synthase or Complex V, NADH-ubiquinone oxidoreductase, succinate dehydrogenase, ubiquinol-cytochrome c reductase, and cytochrome

Abbreviations: OXPHOS, oxidative phosphorylation; ETC, electron transport chain; 3-OHbk, 3-hydroxybakuchiol; MPTP, mitochondrial permeability transport pore; HKII, hexokinase II; VDAC, voltage-dependent anion channel; glucose-6-P, glucose-6-phosphate; NADH, reduced nicotinamide adenine dinucleotide; DQ, duroquinol; DMEM, Dulbecco's Modified Eagle Medium; PBS, phosphate buffered saline; FITC, fluorescein isothiocyanate; DMSO, dimethyl sulfoxide; PI, propidium iodide; FACS, fluorescence-activated cell sorting; TUNEL, terminal deoxyuridine triphosphate nick end labeling; TMRM, tetramethylrhodamine methyl ester; RFU, relative fluorescence units; EGTA, ethylene glycol tetraacetic acid; DCFDA, dichlorofluorescein diacetate; ROS, reactive oxygen species; SEM, standard error of the mean; SD, standard deviation; ANOVA, analysis of variance; CsA, Cyclosporine A; G + M, glutamate plus malate; DEVDase, caspase-3-like enzyme.

* Corresponding author at: Program of Clinical and Molecular Pharmacology, Faculty of Medicine, University of Chile, Independencia 1027, Independencia 8380453, Santiago, RM, Chile. Fax: +56 2 27355580.
E-mail address: jferreir@med.uchile.cl (J. Ferreira).

0041-008X/$ – see front matter © 2013 Elsevier Inc. All rights reserved.
http://dx.doi.org/10.1016/j.taap.2013.06.005

c oxidase are decreased (López-Ríos et al., 2007). The respiration rate in cancer cells is also lower than in normal cells, most likely due to mitochondrial dysfunction (DeBerardinis et al., 2008). Due to the Warburg Effect, several researchers have assumed that glycolysis is the predominant ATP supplier for energy-dependent processes in cancer cells. However, chemotherapeutic strategies using only glycolysis inhibitors have been unsuccessful in arresting tumor proliferation (Rodriguez-Enriquez et al., 2012). For these reasons, finding molecules capable of inhibiting OXPHOS in tumor cells is an urgent priority.

Bakuchiol (Fig. 1A) is a prenylated monoterpene isolated from the seeds of *Psoralea corylifolia* and *Psoralea glandulosa* (Leguminosae) (Labbé et al., 1996). This compound has been used in the treatment of several diseases in traditional Chinese medicine. Bakuchiol inhibits iNOS and has antibacterial, antioxidant, antitumor, and anti-inflammatory activities (Adhikari et al., 2003; Bapat et al., 2005; Katsura et al., 2001; Pae et al., 2001; Sun et al., 1998). Bakuchiol also induces apoptosis in different cellular models, such as rat liver myofibroblasts (Park et al., 2007) and cancer cells (Chen et al., 2010). In our search for new anticancer molecules, we found several catechols that kill neoplastic cells by inhibiting mitochondrial respiration and depleting intracellular pools of ATP (Plaza et al., 2008). A similar isoprenylated catechol, 3-hydroxybakuchiol (3-OHbk), was isolated from the Chilean plant *P. glandulosa*, in which the compound is present in extremely small amounts (Labbé et al., 1996). Only one synthesis route for this compound has been described to date (Perales et al., 2002). 3-OHbk shares most of its structure with bakuchiol but has a hydroxyl group on carbon 3 of the aromatic ring (Labbé et al., 1996). Due to its catecholic nature, 3-OHbk can react with several intracellular targets (as do other polyphenols), including mitochondrial proteins. In the current study, we showed that 3-OHbk has a better antiproliferative effect than bakuchiol and induces apoptosis by inhibiting the electron flow at the Complex I level and by activating a mitochondria-dependent death pathway.

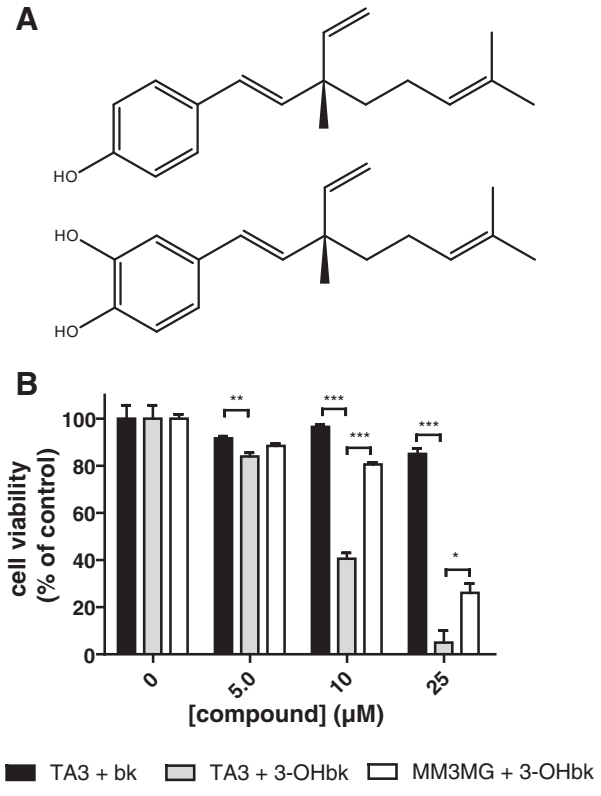

Fig. 1. 3-Hydroxybakuchiol has a greater antiproliferative effect on TA3 tumor cells than bakuchiol. A) Chemical structures of bakuchiol and 3-hydroxybakuchiol. B) TA3 (10^4 cells/well) and MM3MG (4×10^3) cells were seeded in 96-well plates and treated with 3-hydroxybakuchiol, bakuchiol, or DMSO for 48 h. Cell proliferation was assessed with the neutral red assay. The results are expressed as a percentage of the control (DMSO) values and represent the mean ± SEM of at least three independent experiments. $^*P < 0.05$, $^{**}P < 0.01$, $^{***}P < 0.001$.

Methods

Chemicals. Bakuchiol and 3-hydroxybakuchiol were isolated previously (Labbé et al., 1996). Duroquinol was reduced from duroquinone immediately before use, as previously described (Plaza et al., 2008).

Cell lines. The MM3MG mouse mammary epithelial cell line was purchased from the American Type Culture Collection (ATCC, Catalog No. CRL 6376, Manassas, VA). The TA3/Ha mouse mammary adenocarcinoma line was kindly provided by Dr. Gasic, University of Pennsylvania, and has been used by our laboratory since 1989 (Fones et al., 1989). TA3/Ha cells were maintained in ascites fluid by i.p. inoculation (1×10^6 cell/0.1 ml) into 7- to 9-week-old CAF1/J mice as previously described (Fung et al., 1990). The mice were purchased from the animal facility of the Faculty of Medicine of the University of Chile, where they were housed and fed under the same conditions as previously described (Plaza et al., 2008). The University of Chile Committee on Animal Welfare approved all animal protocols used in this study, and all precautions were taken to ensure that the animals did not suffer unduly.

Cell cultures. The MM3MG and TA3/Ha cell lines were grown in high-glucose DMEM supplemented with 10% fetal bovine serum, penicillin (100 IU/ml), and streptomycin (100 μg/ml) in an incubator with a humidified atmosphere at 5% CO_2 and 37 °C.

Isolation of mitochondria from TA3/Ha cells. Mitochondrial suspensions of approximately 20 mg protein/ml were prepared from tumor cells as described previously (Moreadith and Fiskum, 1984), with the following minor modifications: the mitochondrial fractions were washed twice at 12,000 ×*g* for 10 min and re-suspended in a minimal volume of their respective medium in the absence of bovine serum albumin to eliminate hydrophobic compound adsorption. The protein concentration was determined by the Lowry assay (Lowry et al., 1951).

Antiproliferative assay. 3-OHbk and bakuchiol were dissolved in DMSO and diluted in fresh medium to the indicated concentrations. The final concentration of DMSO in the incubation medium was 0.1%. MM3MG (4×10^3 cells/well) and TA3/Ha (1×10^4 cells/well) cells were seeded in 96-well plates and allowed to grow for 24 h at 37 °C in a humidified atmosphere at 5% CO_2. Then, the culture medium was replaced with fresh medium containing increasing concentrations of either 3-OHbk or bakuchiol, and the cells were allowed to grow for 48 h. Then, the cells were subjected to the neutral red assay to estimate the number of viable cells, as described previously (Repetto et al., 2008). Briefly, the cell samples were washed two times with PBS and incubated with 0.1 mg/ml neutral red for 1 h. Then, the cells were washed three times to remove the unincorporated neutral red and solubilized with acidic ethanol. The absorbance was measured at 540 nm. The data are represented as a percentage of the control value from three independent experiments.

Cell death assay. Cell death was assessed as previously described (Syed et al., 2012). The Annexin V-fluorescein isothiocyanate (Annexin V-FITC) and propidium iodide (PI) labeling was performed with the Apoptosis/Necrosis Detection Kit (Abcam, UK) according to the manufacturer's instructions. After 24 h of treatment, the cells were harvested, and Annexin V-FITC was added to a final concentration of 2.5 mg/ml. To detect necrotic cells, PI was added at a concentration of 5 mg/ml. The Annexin V-FITC and PI-labeled cells were analyzed by FACS (FACS Canto, BD Biosciences, San Jose, CA, USA). Using flow cytometry, dot plots of Annexin V-FITC on the X-axis against PI on the Y-axis were used to distinguish viable cells (which are negative for both PI and Annexin V-FITC), early apoptotic cells (which are Annexin V positive but PI negative) and late apoptotic or necrotic cells (which

are positive for both PI and Annexin V-FITC staining). Unstained cells and untreated cells were used as negative controls. The data were analyzed using Cyflogic software (non-commercial version, CyFlo Ltd.).

TUNEL assay. Cells undergoing DNA fragmentation were assessed by the DeadEnd™ Fluorometric TUNEL System (Promega, USA) according to the manufacturer's instructions and were visualized using a Nikon Eclipse E400 epifluorescence microscope. Digital images of terminal deoxyuridine triphosphate nick end labeling (TUNEL) and nuclear morphology were obtained using a Digital DS-Ri1 Nikon camera. The TUNEL results were determined by scoring at least 500 cells as previously described (Duaso et al., 2011). The data are expressed as the percentage of TUNEL-positive cells relative to total cells.

Cell cycle analysis. For cell cycle analysis, TA3/Ha cells were cultured in 24 well plate (10^5 cells/well), with or without 3-OHbk at the indicated concentrations for 24 h. Cells were then harvested, washed in PBS and permeabilized with methanol, then were washed in PBS, and resuspended in 1 mL of 0.1% sodium citrate containing 0.05 mg of PI and 50 μg of RNase for 30 min at room temperature in the dark. Flow cytometry was performed on FACS Canto (BD Biosciences), with collection and analysis of data performed using CellQuest Software (BD Biosciences).

Caspase-3 activity assay. Colorimetric assay kits (Sigma Aldrich, USA) were used to measure the enzyme activity of caspase-3 according to the manufacturer's instructions. Cytoplasmic protein (150 μg) extracted from cells treated with bakuchiol and colorimetric substrate (5 μl) was added to 50 μl of reaction buffer. The mixture was placed in a 96-well plate and incubated for 1 h at 37 °C. The absorbance at 405 nm was measured. Caspase activity was expressed as a percentage of the control value from three independent experiments.

Mitochondrial potential determination. To determine the change in the mitochondrial potential, vehicle- and 3-OHbk-treated TA3/Ha cells were exposed to 100 nM of tetramethylrhodamine methyl ester (TMRM) (Invitrogen) for 20 min at 37 °C. The fluorescence was analyzed by flow cytometry. The data are expressed in relative fluorescence units (RFU) and are the means of three independent experiments.

ATP levels. The intracellular ATP levels were determined using the CellTiter-Glo® luciferin/luciferase assay (Promega, USA) according to the manufacturer's instructions using a multiwell luminometer Thermo MultiScan as previously described (Chiong et al., 2010). The data are expressed as a percentage of the control value from at least three independent experiments.

Mitochondrial swelling assay. To assess mitochondrial swelling, changes in side scatter at 540 ± 1 nm of a 0.5 mg/ml suspension of mitochondria in experimental buffer (125 mM KCl, 10 mM Tris–HCl [pH 7.4], 1 mM Pi, 5 mM glutamate, 2.5 mM malate, and 10 μM EGTA-Tris [pH 7.4]) were monitored using a JASCO V-560 UV/VIS Spectrophotometer (Fantin et al., 2002). The data are expressed as the difference in the absorbance before and after the addition of the stimulus. Each point corresponds to the mean ± SEM of three independent experiments.

Oxygen consumption determination in isolated mitochondria. The rates of oxygen consumption were measured polarographically at 25 °C with a No. 5331 Clark-type electrode (Yellow Springs Instrument, Yellow Spring, OH, USA) using a YSI model 5300 monitor (Yellow Springs Instrument, Yellow Spring, OH, USA) linked to a DI-148U data acquisition module with a USB interface. The data were acquired with Windaq Acquisition Waveform Recorder software (DataQ Instruments, USA). The 0.6 ml reaction contained final concentrations of 200 mM sucrose, 50 mM KCl, 3 mM Hepes (pH 7.4), 0.5 mM EGTA, 3 mM potassium phosphate, 2 mM $MgCl_2$, and 0.5 mg/ml of mitochondrial protein. The system was equilibrated with mitochondria at 25 °C, and then 2.5 mM glutamate with 2.5 mM malate, 5 mM succinate, or 1 mM duroquinol as respiration substrates was added two minutes later. After incubation at 25 °C for 1 min, 3-OHbk was added at the indicated concentrations, then 175 μM ADP was added one minute later, and the oxygen consumption rate due to state 3 respiration was measured (Okuda et al., 2010). The data correspond to the mean of the percentage of the respiration rate relative to the basal respiration rate in three independent experiments.

ROS determination. The intracellular sensor dichlorofluorescein diacetate (DCFDA, Sigma-Aldrich, USA) was used to measure the reactive oxygen species (ROS) production in TA3/Ha cells (2.5×10^4 cells/well). The cells were incubated with DCFDA (20 μM, 15 min, 37 °C) in DMEM and then washed and re-suspended in PBS (pH 7.4). The fluorescence was measured using a BioTek Synergy HT spectrofluorimeter (EX 488 nm, EM 528 nm). Data were obtained and analyzed with Gen5 (BioTek, USA). The data are represented as the slope of the increase in the level of fluorescence (RFU/min).

Statistical analysis. All results were expressed as the mean values ± SEM. Statistically significant differences were identified using Student's *t* test or one-way ANOVA. $P < 0.05$ was considered statistically significant.

Results

Bakuchiol and 3-hydroxybakuchiol have antiproliferative effects on TA3/Ha tumor cells

Both bakuchiol and 3-hydroxybakuchiol exhibited concentration-dependent antiproliferative effects on mouse mammary adenocarcinoma TA3/Ha cells as assessed by the neutral red assay (Repetto et al., 2008). However, 3-hydroxybakuchiol had a more potent effect than bakuchiol (IC_{50} of 8.25 ± 1.06 μM and 42.6 ± 1.07 μM for 3-hydroxybakuchiol and bakuchiol, respectively). The antiproliferative effect of 3-OHbk was less pronounced when using the normal epithelial MM3MG cell line (Fig. 1B).

3-Hydroxybakuchiol induces apoptosis in TA3/Ha cells

There is evidence suggesting that bakuchiol induces apoptosis in tumor cells (Bapat et al., 2005; Chen et al., 2010). However, as a result of the greater antiproliferative effects of 3-OHbk on the TA3/Ha cell line, we assessed the effect of this compound on cell death induction. After the incubation of TA3/Ha and MM3MG cells with increasing concentrations of 3-OHbk for 24 h, annexin V-positive apoptotic cells were observed among TA3/Ha cells (Figs. 2A and B) but not in MM3MG cells (Fig. 2C). Additionally, apoptotic DNA fragmentation (Loo, 2011) was assessed in TA3/Ha cells exposed to 3-OHbk for 1 and 4 h. As shown in Figs. 2D and E, there was a 25% increase in the percentage of TUNEL-positive cells as the concentration of 3-OHbk increased from 10 to 20 μM, showing that, as early as 4 h of incubation with 3-OHbk, DNA fragmentation is observed. Furthermore, no significant accumulation of events was observed in any specific stage of the cell cycle; however, there was a significant increase in subG1 population (Fig. 2F), confirming the early DNA fragmentation observed in TUNEL assay (Fig. 2D).

The activation of caspases is a critical event in the induction of apoptosis. Thus, we measured the caspase-3-like enzyme (DEVDase) activity through a colorimetric assay with Ac-DEVD-pNA as the substrate. Caspase-3-like enzyme activity was increased by 50% after exposure to 20 μM 3-OHbk for 4 h (Fig. 2G).

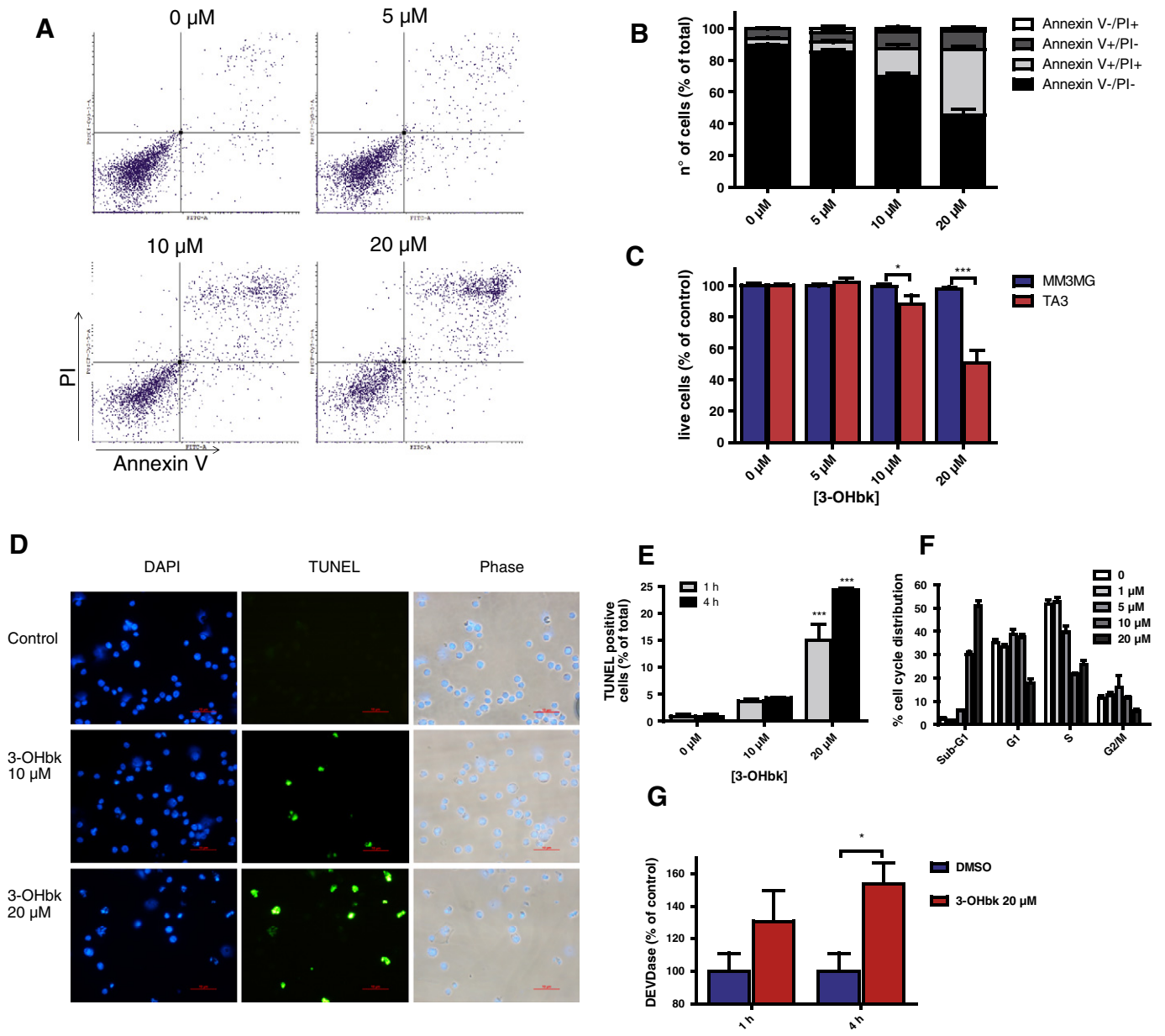

Fig. 2. 3-OHbk induces apoptosis in the TA3 tumor cell line but not in the MM3MG normal cell line. A) TA3 cells were seeded in a 24-well plate (10^5 cells/well). After 24 h, the cells were exposed to the indicated concentrations of 3-OHbk for 24 h, and PI and Annexin V incorporation in 10,000 cells was analyzed by flow cytometry. B) The values represented as the percentages in each quadrant from A are plotted. Black bars represent live cells. C) Annexin V binding and PI incorporation were assessed in TA3 and MM3MG cells under the same conditions as in A), and live cells (annexin V^-/PI^-) are shown. D) TA3 cells (10^4 cells/well) were plated in a 96-well plate and exposed to 3-OHbk at the indicated concentration for 4 h. Then, the terminal deoxynucleotidyl transferase activity (TdT) was measured by the TUNEL fluorometric assay. Representative images from at least three independent experiments are shown. Bar = 100 μm. E) The percentage of TUNEL-positive cells, relative to the total cells, after 1 and 4 h of incubation with 3-OHbk are shown. F) TA3 cells were seeded in a 24-well plate (10^5 cells/well). After 24 h, the cells were exposed to the indicated concentrations of 3-OHbk for 24 h, and the DNA content of 10,000 cells was analyzed by flow cytometry. The proportions (%) of cells in each phase are shown. G) TA3 cells were seeded in a 100 mm diameter petri dish (10^6 cells/plate) and exposed to 3-OHbk at the indicated concentrations for 1 and 4 h. Caspase 3-like activity was measured by a colorimetric assay using the DEVD-pNA substrate. All data correspond to the mean ± SEM of at least three independent experiments. $^*P < 0.05$, $^{**}P < 0.01$, $^{***}P < 0.001$.

3-Hydroxybakuchiol induces mitochondrial dysfunction

To determine if the observed cell death was preceded by mitochondrial dysfunction, we measured the mitochondrial transmembrane potential as an indicator of mitochondrial function. The incubation of TA3/Ha cells with 20 μM 3-OHbk resulted in a gradual decrease in the TMRM fluorescence (Fig. 3A). In addition, we assessed the aperture of the mitochondrial permeability transition pore (MPTP) in mitochondria isolated from TA3/Ha cells. At a concentration of 20 μM, 3-OHbk added to the mitochondrial suspension produced mitochondrial swelling (resulting in a decreased absorbance), and this effect was reversed with the addition of 2 μM CsA, a specific MPTP inhibitor (Fig. 3B, left panel). Thus, mitochondrial swelling is explained by MPTP opening and was concentration dependent (Fig. 3B, left panel). The co-incubation of TA3/Ha cells with CsA did not prevent 3-OHbk-induced cell death (Fig. 3B, right panel). Therefore, the cell death induced by 3-OHbk does not rely exclusively on MPTP opening. However, as expected, the intracellular ATP levels fell dramatically in TA3/Ha cells incubated with 20 μM 3-OHbk, while non-cancerous cells MM3MG were less affected (Fig. 3C).

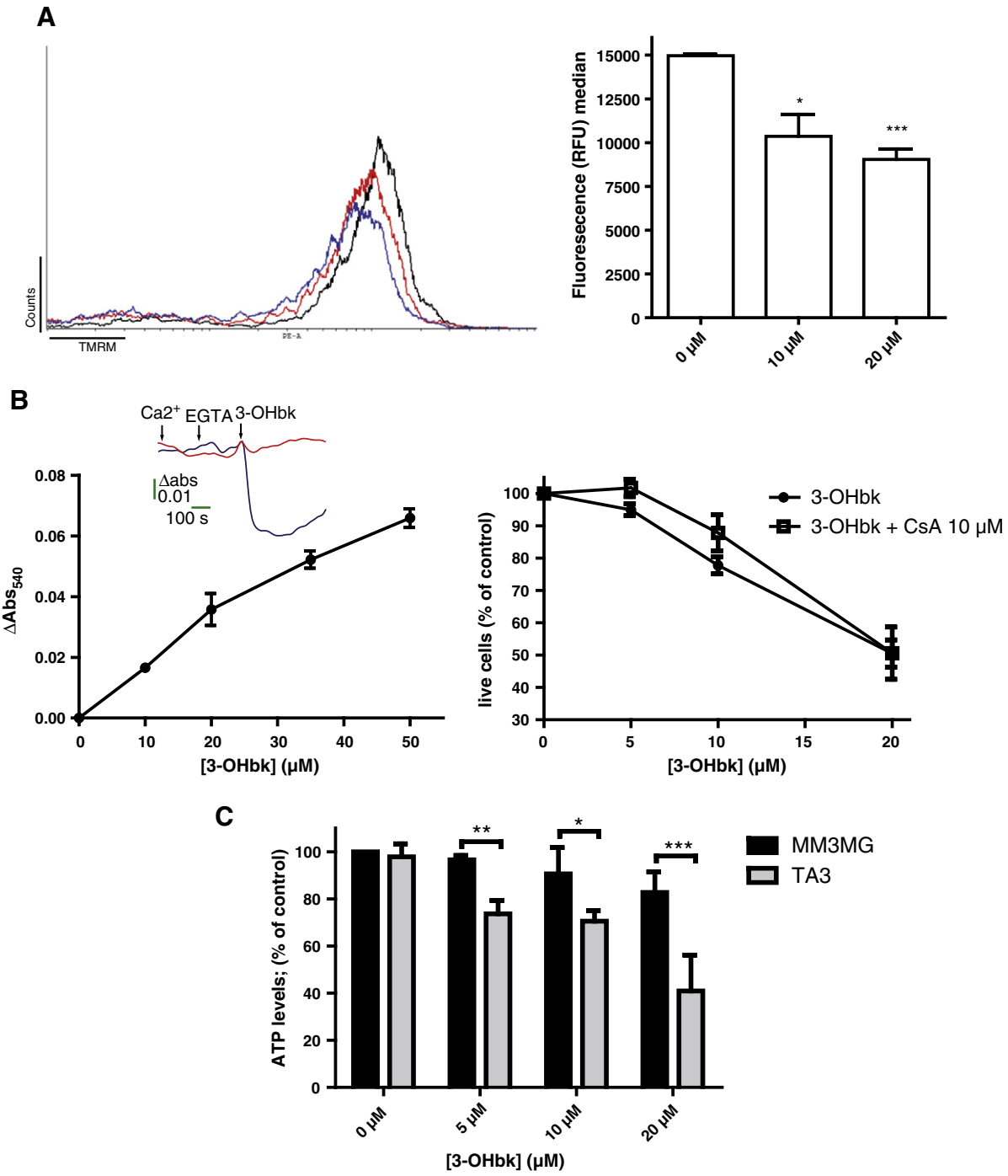

Fig. 3. 3-OHbk induces mitochondrial dysfunction in TA3 cells. A) TA3 cells (10^5 cells/well) were seeded in a 24-well plate and exposed to DMSO, 10 μM 3-OHbk or 20 μM 3-OHbk for 4 h (black, red, and blue lines, respectively). Then, TA3 cells were incubated with TMRM for 15 min, and the red fluorescence was analyzed by flow cytometry. The left panel shows a representative histogram of three independent experiments, quantified in the right panel. B) Isolated tumor cell mitochondria (0.5 mg/ml protein) were pre-incubated with Ca^{2+}. Then, 20 μM 3-OHbk was added. The absorbance at 540 nm was measured after 15 min, and the difference between the absorbance of the mitochondrial suspension before and after the addition of 3-OHbk was quantified. The right panel shows the percentage of annexin V-/PI- (live) cells among 10^5 cells incubated with the indicated concentrations of 3-OHbk for 24 h in the presence of 10 μM CsA or vehicle. C) TA3 or MM3MG cell lines (10^4 cells/well) were seeded in a 96-well plate and incubated with the indicated concentrations of 3-OHbk for 4 h. Later, a 100 μL aliquot was extracted from each well and mixed with 100 μL of reaction buffer of a luciferin/luciferase-based assay. The luminescence was read using a multi-well luminometer. The data correspond to the mean ± SEM of at least three independent experiments. $^*P < 0.05$, $^{**}P < 0.01$, $^{***}P < 0.001$.

3-Hydroxybakuchiol disrupts the mitochondrial electron transport chain in TA3/Ha cells

To determine if the mitochondrial dysfunction is due to alterations in the mitochondrial electron transport chain (ETC) of tumor cells, we studied the effect of 3-OHbk treatment on oxygen consumption in isolated mitochondria from TA3/Ha cells as a measure of electron flow. 3-OHbk inhibited oxygen consumption by up to approximately 80% in glutamate plus malate (G + M)-dependent, ADP-stimulated respiring mitochondria (state 3) in a concentration-dependent manner (Figs. 4A and B). However, the inhibition of oxygen consumption inhibition was not observed when succinate, a substrate that delivers

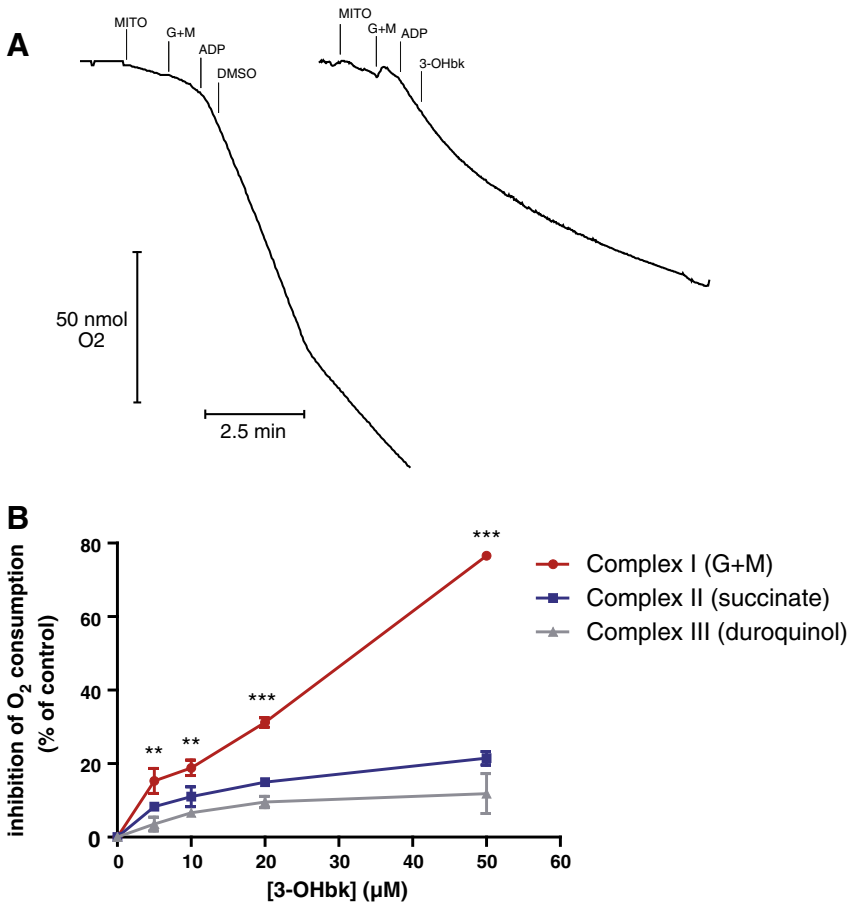

Fig. 4. 3-OHbk inhibits ETC activity. A) Representative curves of the oxygen consumption of a mitochondrial suspension are presented. The oxygen consumption rate was assessed in a 0.6 ml chamber coupled with a Clark-type electrode, and the slope of state 3 respiration (after ADP addition) was calculated. B) A mitochondrial suspension (MITO = 0.3 mg of mitochondrial protein) was incubated with 2.5 mM glutamate with the addition of 2.5 mM malate (G + M), 5 mM succinate, or 1 mM duroquinol, and then the indicated concentrations of 3-OHbk were added. The percentage of oxygen consumption inhibition induced by 3-OHbk relative to the control (DMSO) is presented. All data represent the mean ± SEM of at least three independent experiments.

electrons directly to Complex II, or duroquinol, which delivers electrons directly to Complex III (Fig. 4B) was added (Ray et al., 1994). Thus, given that G + M donates electrons to Complex I, these findings suggest that 3-OHbk disrupts the mitochondrial electron flow through Complex I of the mitochondrial respiratory chain.

Role of ROS in the TA3/Ha cell death induced by 3-hydroxybakuchiol

Several ETC inhibitors induce apoptosis in cancer cells due to ROS generation. Thus, we assessed the effects of 3-OHbk on the induction of ROS generation as a consequence of its ETC inhibition properties. Rotenone is a classic Complex I inhibitor that increases ROS production as detected by dichlorofluorescein oxidation (DCF). However, we did not detect an increase in ROS production in TA3/Ha cells at the 3-OHbk concentrations tested (Fig. 5A). Furthermore, TA3/Ha cells treated with the combination of 3-OHbk and 50 μM rotenone exhibited lower levels of ROS than those induced by 50 μM of rotenone alone (Fig. 5A). Thus, 3-OHbk might have an antioxidant effect. To confirm that ROS are not involved in the cell death induced by 3-OHbk, we co-incubated TA3/Ha cells with 3-OHbk and the antioxidant Trolox®. The results show that co-incubation with Trolox did not decrease the live cell population (Fig. 5B). Therefore, Trolox® scavenged ROS species are not involved in the TA3/Ha cell death induced by 3-OHbk.

Effect of the restoration of electron flow on TA3/Ha cell death induced by 3-hydroxybakuchiol

Given that 3-OHbk disrupts Complex I in the mitochondrial ETC (Fig. 4B), we investigated the effect of this compound on cell death by delivering electrons directly to Complex III in the ETC with duroquinol, thus reversing the inhibitory effect of 3-OHbk on mitochondrial respiration. Although 20 μM 3-OHbk induced death in 50% of the TA3/Ha cell population (Fig. 6A), co-incubation with duroquinol significantly reduced the Annexin V^+/PI^+ population induced by 3-OHbk after 24 h of incubation (Fig. 6B).

Discussion

A growing body of evidence suggests that cancer cells have decreased mitochondrial activity due to the downregulation of aerobic mitochondrial metabolism (Solaini et al., 2011). This downregulation switches ATP generation to the aerobic glycolysis pathway, providing the building blocks necessary for the uncontrolled proliferation of tumor cells (Jose et al., 2011).

The flexibility in ATP generation is an example of the complex relationship between the glycolytic pathway and the OXPHOS system involved in improving energy generation in response to changes in the environment and to the differences in energy or biosynthetic

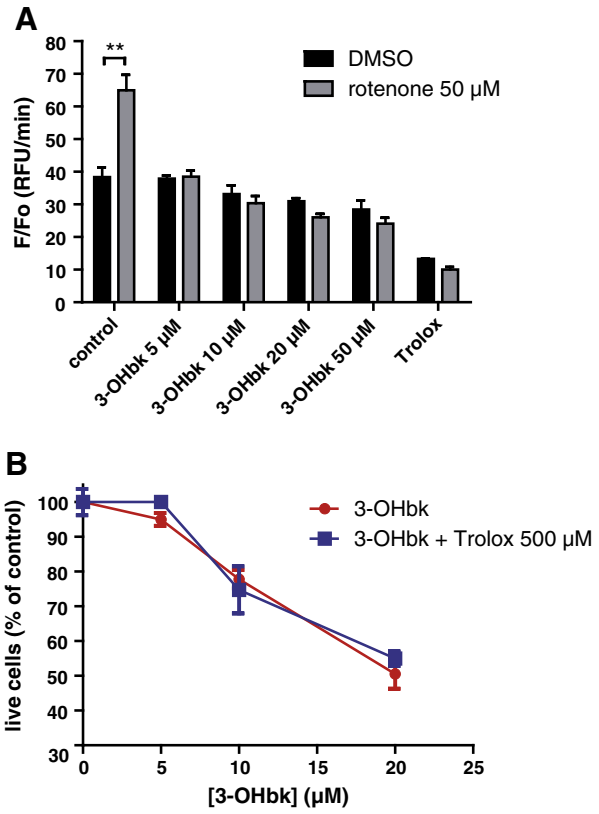

Fig. 5. Effect of 3-OHbk on ROS generation in TA3 cells. A) TA3 cells (2. × 10^5 cells/well) were incubated with DCFDA (20 μM) for 15 min and exposed to the indicated concentrations of 3-OHbk. The level of DCFDA fluorescence was measured immediately in a multi-well fluorimeter (EX. 488 nm, EM. 528 nm) for 40 min. Rotenone (specific Complex I inhibitor) and the antioxidant Trolox were used as positive and negative controls, respectively. B) The chart shows the percentage of annexin V^-/PI^- (live) cells among 10^5 cells/well incubated with the indicated concentrations of 3-OHbk for 24 h in the presence of Trolox® 500 μM or vehicle. All data represent the mean ± SEM of at least three independent experiments.

requirements of tumors. It has also been demonstrated that a variety of human and mouse tumor cell lines use mitochondrial respiration to sustain proliferation. Recently, the measurement of the contribution of OXPHOS to ATP generation in HeLa cells showed that mitochondria generate 79% of cellular ATP and that this contribution is decreased to 30% in hypoxic conditions (Rodriguez-Enriquez et al., 2010). Again, metabolic flexibility is utilized to survive under hypoxic conditions. All of these studies show that the mitochondria efficiently synthesize ATP in a variety of cancer cells (Moreno-Sánchez et al., 2007). Although there is a reduction in the mitochondrial mass in some tumors (Formentini et al., 2010; Isidoro et al., 2004; Sanchez-Arago et al., 2010), cancer cells retain the ability to use OXPHOS instead of glycolysis during carcinogenesis. This change is also observed at the level of the oxidation of glutamine, which occurs as the result of OXPHOS or an anoxic process, allowing the generation of energy from glutamine or serine regardless of hypoxia or reduced ETC activity (Jose et al., 2011; Smolkova et al., 2011).

Therefore, efforts have been made to block only the glycolysis pathway rather than block both this pathway and the OXPHOS system in cancer cells. Due to the dependence of hexokinase II on mitochondrial ATP (Mathupala et al., 2009; Pedersen, 2007), the ETC is also crucial in cancer cells and has proven to be a promising therapeutic target (Solaini et al., 2011). Herein, we demonstrated that a structural analog of the well-known compound bakuchiol, 3-OHbk, has greater antiproliferative activity against the murine mammary adenocarcinoma TA3/Ha cell line. 3-OHbk selectively induces cell death in TA3/Ha cells (Fig. 1B), promoting mitochondrial dysfunction (Fig. 3) and apoptosis, as demonstrated by DNA fragmentation, caspase-3 activation, and phosphatidylserine exposure (Fig. 2). Therefore, 3-OHbk could be a suitable inducer of cell death in tumor cells because this type of cell death prevents inflammatory reactions in the host (Galluzzi et al., 2012). Moreover, as a resveratrol analog (Chen et al., 2010), it is possible that 3-OHbk also could lead to SirT1 activation. Experiments to dilucidate it will be done.

In addition, quinones and polyphenols have been reported to induce apoptosis in tumor cells through ROS generation (Bair et al., 2010; Kovacic and Somanathan, 2011; Kumar et al., 2009; Sagar and Green, 2009; Simamura et al., 2006; Srinivas et al., 2007), possibly through the activation of caspases and other targets, decreasing glutathione (GHS) levels and activating the Jun kinase pathway (JNK) (Curtin et al., 2002; Higuchi, 2004; Koka et al., 2010), among other mechanisms. However, 3-OHbk did not induce ROS in our model. Thus, there are different explanations for the induction of cell death by the polyphenol 3-OHbk. Therefore, we determined whether the inhibition of the electron flow through ETC could be responsible for this phenomenon.

We have shown in TA3/Ha cells that 3-OHbk disrupts the electron flow, acting at the level of Complex I, thus decreasing the rate of oxygen consumption and intracellular ATP levels (Figs. 3B and C). Indeed, in cells derived from other aggressive human metastatic carcinomas (HeLa, CRL 1420 pancreatic, breast MCF-7, and MB49 bladder cells) and in osteosarcoma tumor cells, inhibitors of OXPHOS, such as casiopeina II-gly and rhodamines (123, 6G), also restrict the electron flow through the mitochondrial ETC, with a consequent reduction in the tumor proliferation rate (Moreno-Sánchez et al., 2007). Therefore, it is not surprising that a polyphenol such as 3-OHbk, which inhibits the electron flow, also induces cell death in TA3/Ha tumor cells.

Concomitantly, we observed a decrease in the $\Delta\Psi m$, most likely due to the opening of the MPTP. The small aperture normally inhibits the electron flow through the ETC, due to the leakage of adenine nucleotides from the mitochondrial inner space into the cytoplasm (Fantin et al., 2002). Nevertheless, the opening of the MPTP may not be the reason that 3-OHbk inhibited OXPHOS because the co-incubation of mitochondria with CsA, a specific inhibitor of MPTP, did not prevent the inhibition of oxygen consumption (data not shown) or the TA3/Ha cell death induced by 3-OHbk (Fig. 3B).

Most Complex I inhibitors induce ROS generation, as is the case for the specific Complex I inhibitor rotenone (Moreno-Sánchez et al., 2007) when it is added to TA3/Ha cells (Fig. 5A). However, ROS production, as assessed by DCF oxidation, was not detected in 3-OHbk-treated TA3/Ha cells. This phenomenon might be explained by the polyphenolic nature of 3-OHbk (as catecholic motif), which gives this compound antioxidant properties, thus preventing any DCF oxidation by ROS that it might be generated by the inhibition of Complex I. In addition, co-incubation with Trolox®, a ROS scavenger, did not protect TA3/Ha cells from cell death induced by 3-OHbk (Fig. 5B). Therefore, the cell death induced by 3-OHbk is most likely due to another cause. Nevertheless, the reasons why 3-OHbk did not induce the production of ROS and why this catechol induces apoptosis in cancer cells remain unclear.

A widely accepted mechanism that explains the interaction of several catechols with proteins and other targets are the previous oxidation of the catechol to a quinone and the consequent covalent interaction of the quinone with the thiol groups present in proteins, especially in the mitochondrial respiratory complexes (Gautam and Zeevalk, 2011). For this reason, likely, duroquinol, a membrane-permeable downstream substrate of the ETC, prevents the death of 3-OHbk-treated TA3/Ha cells. Duroquinol delivers electrons directly to Complex III (Plaza et al., 2008), bypassing the 3-OHbk-inhibited Complex I and restoring electron flux through the ETC (Fig. 4B). Thus, the inhibition of Complex I and the consequent inhibition of oxygen consumption are the direct cause of the cell death induced by 3-OHbk. This electron flow inhibition decreases the $\Delta\Psi m$, probably by the diminished proton pumping through Complexes I, III and IV, leading to a MPTP activation and the consequent mitochondrial dysfunction.

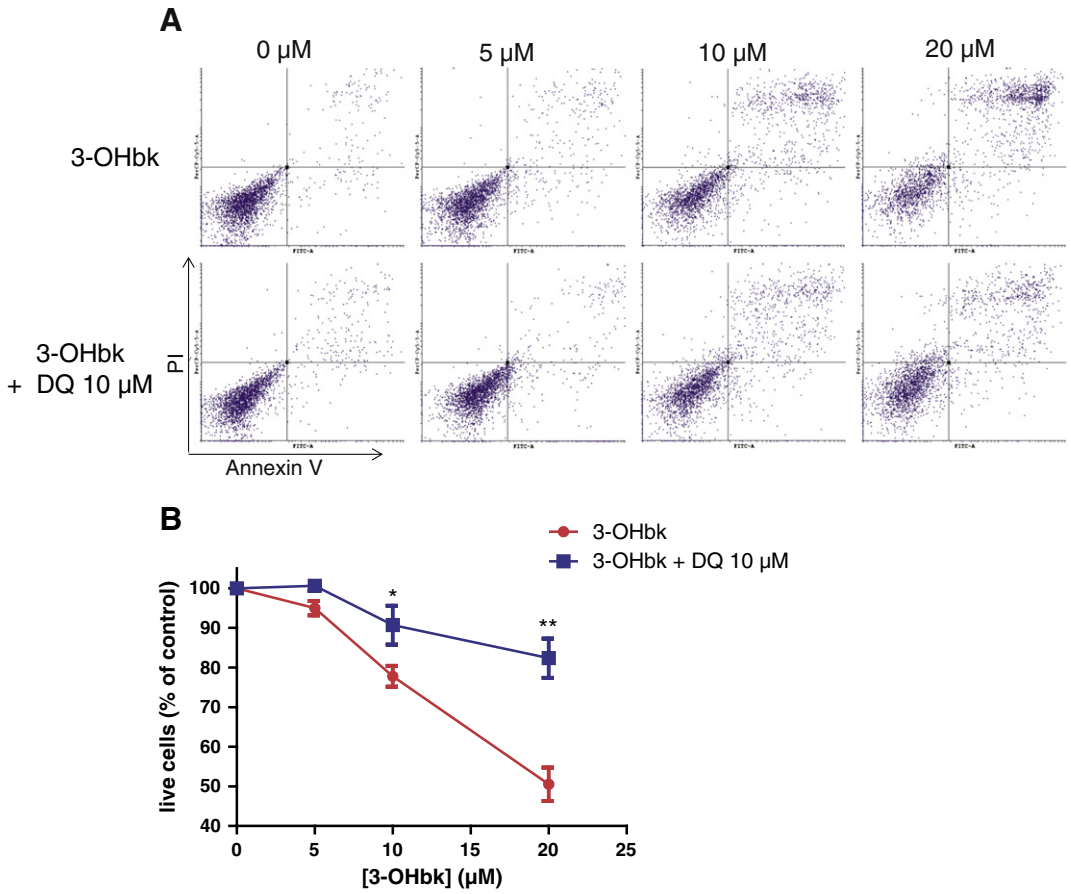

Fig. 6. Duroquinol prevents TA3 cell death induced by 3-OHbk. A) 10^5 cells/well were seeded in a 24-well plate and exposed to the indicated concentrations of 3-OHbk in the presence of 10 μM duroquinol or vehicle. Then, annexin V binding and PI incorporation were assessed by flow cytometry. BN The events that represent annexin V^-/PI^- (live cells) are plotted as a percentage of the control values. All data are the means ± SEM of at least three independent experiments.

This will lead to liberation of pro-apoptotic factors which will activate caspase 3, and an induction of DNA fragmentation, leading to an apoptotic cell death. This novel mechanism promotes apoptotic cell death through ATP depletion only in the cancerous cell line, instead of ROS generation, thus preventing the unwanted effects produced by ROS. However, the mechanism for the selectivity on ATP depletion for tumor cells has not been yet elucidated.

The evidence provided by this study suggests that 3-OHbk has antiproliferative activity in tumor cells. This effect can be explained by the induction of apoptosis as a consequence of the inhibition of electron flow in the mitochondria at the Complex I level. However, altering the OXPHOS system alone is not sufficient to cause a complete antineoplastic effect, therefore, studies of the effect of 3-OHbk on the glycolysis of mammary adenocarcinoma cells TA3/Ha must be made.

Moreover, further studies are needed to provide evidence of this antitumor effect in vivo and to verify the selectivity of this compound.

Competing interests

The authors declare they have no competing interests.

Acknowledgments

This research was funded by FONDECYT 1090075 (JF), 1120230 (UK), Anillo ACT-112 and Ph.D. fellowship CONICYT 21080116 (FJ).

References

Adhikari, S., Joshi, R., Patro, B.S., Ghanty, T.K., Chintalwar, G.J., Sharma, A., Chattopadhyay, S., Mukherjee, T., 2003. Antioxidant activity of bakuchiol: experimental evidences and theoretical treatments on the possible involvement of the terpenoid chain. Chem. Res. Toxicol. 16, 1062–1069.

Bair, J.S., Palchaudhuri, R., Hergenrother, P.J., 2010. Chemistry and biology of deoxynyboquinone, a potent inducer of cancer cell death. J. Am. Chem. Soc. 132, 5469–5478.

Bapat, K., Chintalwar, G.J., Pandey, U., Thakur, V.S., Sarma, H.D., Samuel, G., Pillai, M.R., Chattopadhyay, S., Venkatesh, M., 2005. Preparation and in vitro evaluation of radioiodinated bakuchiol as an anti tumor agent. Appl. Radiat. Isot. 62, 389–393.

Chen, Z., Jin, K., Gao, L., Lou, G., Jin, Y., Yu, Y., Lou, Y., 2010. Anti-tumor effects of bakuchiol, an analogue of resveratrol, on human lung adenocarcinoma A549 cell line. Eur. J. Pharmacol. 643, 170–179.

Chiong, M., Parra, V., Eisner, V., Ibarra, C., Maldonado, C., Criollo, A., Bravo, R., Quiroga, C., Contreras, A., Vicencio, J.M., Cea, P., Bucarey, J.L., Molgo, J., Jaimovich, E., Hidalgo, C., Kroemer, G., Lavandero, S., 2010. Parallel activation of Ca(2+)-induced survival and death pathways in cardiomyocytes by sorbitol-induced hyperosmotic stress. Apoptosis 15, 887–903.

Curtin, J.F., Donovan, M., Cotter, T.G., 2002. Regulation and measurement of oxidative stress in apoptosis. J. Immunol. Methods 265, 49–72.

DeBerardinis, R.J., Cheng, T., 2010. Q's next: the diverse functions of glutamine in metabolism, cell biology and cancer. Oncogene 29, 313–324.

DeBerardinis, R.J., Lum, J.J., Hatzivassiliou, G., Thompson, C.B., 2008. The biology of cancer: metabolic reprogramming fuels cell growth and proliferation. Cell Metab. 7, 11–20.

Duaso, J., Rojo, G., Jana, F., Galanti, N., Cabrera, G., Bosco, C., Lopez-Munoz, R., Maya, J.D., Ferreira, J., Kemmerling, U., 2011. *Trypanosoma cruzi* induces apoptosis in ex vivo infected human chorionic villi. Placenta 32, 356–361.

Fantin, V.R., Berardi, M.J., Scorrano, L., Korsmeyer, S.J., Leder, P., 2002. A novel mitochondriotoxic small molecule that selectively inhibits tumor cell growth. Cancer Cell 2, 29–42.

Fones, E., Amigo, H., Gallegos, K., Guerrero, A., Ferreira, J., 1989. t-Butyl-4-hydroxyanisole as an Inhibitor of tumor-cell respiration. Biochem. Pharmacol. 38, 3443–3451.

Formentini, L., Martinez-Reyes, I., Cuezva, J.M., 2010. The mitochondrial bioenergetic capacity of carcinomas. IUBMB Life 62, 554–560.
Fung, P.Y.S., Madej, M., Koganty, R.R., Longenecker, B.M., 1990. Active specific immunotherapy of a murine mammary adenocarcinoma using a synthetic tumor-associated glycoconjugate. Cancer Res. 50, 4308–4314.
Galluzzi, L., Vitale, I., Abrams, J.M., Alnemri, E.S., Baehrecke, E.H., Blagosklonny, M.V., Dawson, T.M., Dawson, V.L., El-Deiry, W.S., Fulda, S., Gottlieb, E., Green, D.R., Hengartner, M.O., Kepp, O., Knight, R.A., Kumar, S., Lipton, S.A., Lu, X., Madeo, F., Malorni, W., Mehlen, P., Nunez, G., Peter, M.E., Piacentini, M., Rubinsztein, D.C., Shi, Y., Simon, H.U., Vandenabeele, P., White, E., Yuan, J., Zhivotovsky, B., Melino, G., Kroemer, G., 2012. Molecular definitions of cell death subroutines: recommendations of the Nomenclature Committee on Cell Death 2012. Cell Death Differ. 19, 107–120.
Gatenby, R.A., Gillies, R.J., 2004. Why do cancers have high aerobic glycolysis? Nat. Rev. Cancer 4, 891–899.
Gautam, A.H., Zeevalk, G.D., 2011. Characterization of reduced and oxidized dopamine and 3,4-dihydrophenylacetic acid, on brain mitochondrial electron transport chain activities. Biochim. Biophys. Acta 1807, 819–828.
Higuchi, Y., 2004. Glutathione depletion-induced chromosomal DNA fragmentation associated with apoptosis and necrosis. J. Cell. Mol. Med. 8, 455–464.
Isidoro, A., Martínez, M., Fernández, P.L., Ortega, A.D., Santamaría, G., Chamorro, M., Reed, J.C., Cuezva, J.M., 2004. Alteration of the bioenergetic phenotype of mitochondria is a hallmark of breast, gastric, lung and oesophageal cancer. Biochem. J. 378, 17–20.
Jose, C., Bellance, N., Rossignol, R., 2011. Choosing between glycolysis and oxidative phosphorylation: a tumor's dilemma? Biochim. Biophys. Acta 1807, 552–561.
Katsura, H., Tsukiyama, R.I., Suzuki, A., Kobayashi, M., 2001. In vitro antimicrobial activities of bakuchiol against oral microorganisms. Antimicrob. Agents Chemother. 45, 3009–3013.
Koka, P.S., Mondal, D., Schultz, M., Abdel-Mageed, A.B., Agrawal, K.C., 2010. Studies on molecular mechanisms of growth inhibitory effects of thymoquinone against prostate cancer cells: role of reactive oxygen species. Exp. Biol. Med. 235, 751–760.
Kovacic, P., Somanathan, R., 2011. Recent developments in the mechanism of anticancer agents based on electron transfer, reactive oxygen species and oxidative stress. Anticancer Agents Med. Chem. 11, 658–668.
Kroemer, G., Pouyssegur, J., 2008. Tumor cell metabolism: cancer's Achilles' heel. Cancer Cell 13, 472–482.
Kumar, M.R., Aithal, K., Rao, B.N., Udupa, N., Rao, B.S., 2009. Cytotoxic, genotoxic and oxidative stress induced by 1,4-naphthoquinone in B16F1 melanoma tumor cells. Toxicol. In Vitro 23, 242–250.
Labbé, C., Faini, F., Coll, J., Connolly, J.D., 1996. Bakuchiol derivatives from the leaves of *Psoralea glandulosa*. Phytochemistry 42, 1299–1303.
Loo, D.T., 2011. In situ detection of apoptosis by the TUNEL assay: an overview of techniques. Methods Mol. Biol. 682, 3–13.
López-Ríos, F., Sánchez-Aragó, M., García-García, E., Ortega, A.D., Berrendero, J.R., Pozo-Rodríguez, F., López-Encuentra, A., Ballestín, C., Cuezva, J.M., 2007. Loss of the mitochondrial bioenergetic capacity underlies the glucose avidity of carcinomas. Cancer Res. 67, 9013–9017.
Lowry, O.H., Rosebrough, N.J., Farr, A.L., Randall, R.J., 1951. Protein measurement with the Folin phenol reagent. J. Biol. Chem. 193, 265–275.
Mathupala, S.P., Ko, Y.H., Pedersen, P.L., 2009. Hexokinase-2 bound to mitochondria: cancer's stygian link to the "Warburg Effect" and a pivotal target for effective therapy. Semin. Cancer Biol. 19, 17–24.
Moreadith, R.W., Fiskum, G., 1984. Isolation of mitochondria from ascites tumor cells permeabilized with digitonin. Anal. Biochem. 137, 360–367.
Moreno-Sánchez, R., Rodríguez-Enríquez, S., Marín-Hernández, A., Saavedra, E., 2007. Energy metabolism in tumor cells. FEBS J. 274, 1393–1418.
Okuda, T., Norioka, M., Shitara, Y., Horie, T., 2010. Multiple mechanisms underlying troglitazone-induced mitochondrial permeability transition. Toxicol. Appl. Pharmacol. 248, 242–248.
Pae, H.O., Cho, H., Oh, G.S., Kim, N.Y., Song, E.K., Kim, Y.C., Yun, Y.G., Kang, C.L., Kim, J.D., Kim, J.M., Chung, H.T., 2001. Bakuchiol from *Psoralea corylifolia* inhibits the expression of inducible nitric oxide synthase gene via the inactivation of nuclear transcription factor-kappa B in RAW 264.7 macrophages. Int. Immunopharmacol. 1, 1849–1855.
Park, E.J., Zhao, Y.Z., Kim, Y.C., Sohn, D.H., 2007. Bakuchiol-induced caspase-3-dependent apoptosis occurs through c-Jun NH2-terminal kinase-mediated mitochondrial translocation of Bax in rat liver myofibroblasts. Eur. J. Pharmacol. 559, 115–123.
Pedersen, P.L., 2007. The cancer cell's "power plants" as promising therapeutic targets: an overview. J. Bioenerg. Biomembr. 39, 1–12.
Pedersen, P.L., 2012. 3-Bromopyruvate (3BP) a fast acting, promising, powerful, specific, and effective "small molecule" anti-cancer agent taken from labside to bedside: introduction to a special issue. J. Bioenerg. Biomembr. 44, 1–6.
Perales, J.B., Makino, N.F., Van Vranken, D.L., 2002. Convergent stereocontrol in Peterson olefinations. Application to the synthesis of (+/−)-3-hydroxybakuchiol and corylifolin. J. Org. Chem. 67, 6711–6717.
Plaza, C., Pavani, M., Faundez, M., Maya, J.D., Morello, A., Becker, M.I., De Ioannes, A., Cumsille, M.A., Ferreira, J., 2008. Inhibitory effect of nordihydroguaiaretic acid and its tetra-acetylated derivative on respiration and growth of adenocarcinoma TA3 and its multiresistant variant TA3MTX-R. In Vivo 22, 353–361.
Ray, S., Dutta, S., Halder, J., Ray, M., 1994. Inhibition of electron flow through complex I of the mitochondrial respiratory chain of Ehrlich ascites carcinoma cells by methylglyoxal. Biochem. J. 303 (Pt 1), 69–72.
Repetto, G., del Peso, A., Zurita, J.L., 2008. Neutral red uptake assay for the estimation of cell viability/cytotoxicity. Nat. Protoc. 3, 1125–1131.
Rodriguez-Enriquez, S., Carreno-Fuentes, L., Gallardo-Perez, J.C., Saavedra, E., Quezada, H., Vega, A., Marin-Hernandez, A., Olin-Sandoval, V., Torres-Marquez, M.E., Moreno-Sanchez, R., 2010. Oxidative phosphorylation is impaired by prolonged hypoxia in breast and possibly in cervix carcinoma. Int. J. Biochem. Cell Biol. 42, 1744–1751.
Rodriguez-Enriquez, S., Gallardo-Perez, J.C., Marin-Hernandez, A., Moreno-Sanchez, R., 2012. The Warburg Hypothesis and the ATP supply in cancer cells. Is oxidative phosphorylation impaired in malignant neoplasias? Curr. Pharm. Biotechnol. 1, 1.
Sagar, S., Green, I.R., 2009. Pro-apoptotic activities of novel synthetic quinones in human cancer cell lines. Cancer Lett. 285, 23–27.
Sanchez-Arago, M., Chamorro, M., Cuezva, J.M., 2010. Selection of cancer cells with repressed mitochondria triggers colon cancer progression. Carcinogenesis 31, 567–576.
Simamura, E., Hirai, K., Shimada, H., Koyama, J., Niwa, Y., Shimizu, S., 2006. Furanonaphthoquinones cause apoptosis of cancer cells by inducing the production of reactive oxygen species by the mitochondrial voltage-dependent anion channel. Cancer Biol. Ther. 5, 1523–1529.
Smolkova, K., Plecita-Hlavata, L., Bellance, N., Benard, G., Rossignol, R., Jezek, P., 2011. Waves of gene regulation suppress and then restore oxidative phosphorylation in cancer cells. Int. J. Biochem. Cell Biol. 43, 950–968.
Solaini, G., Sgarbi, G., Baracca, A., 2011. Oxidative phosphorylation in cancer cells. Biochim. Biophys. Acta 1807, 534–542.
Srinivas, G., Babykutty, S., Sathiadevan, P.P., Srinivas, P., 2007. Molecular mechanism of emodin action: transition from laxative ingredient to an antitumor agent. Med. Res. Rev. 27, 591–608.
Sun, N.J., Woo, S.H., Cassady, J.M., Snapka, R.M., 1998. DNA polymerase and topoisomerase II inhibitors from *Psoralea corylifolia*. J. Nat. Prod. 61, 362–366.
Syed, F., Thomas, A.N., Singh, S., Kolluru, V., Emeigh Hart, S.G., Bayat, A., 2012. In vitro study of novel collagenase (XIAFLEX(R)) on Dupuytren's disease fibroblasts displays unique drug related properties. PLoS One 7, e31430.
Vander Heiden, M.G., Cantley, L.C., Thompson, C.B., 2009. Understanding the Warburg effect: the metabolic requirements of cell proliferation. Science 324, 1029–1033.